J. Biochem. **139**, 837–846 (2006)
doi:10.1093/jb/mvj095

An Efficient RNA Aptamer against Human Influenza B Virus Hemagglutinin

Subash C.B. Gopinath, Yuriko Sakamaki, Kazunori Kawasaki and Penmetcha K.R. Kumar*

Functional Nucleic Acids Group, Institute for Biological Resources and Functions, National Institute of Advanced Industrial Science and Technology (AIST), Central 6, 1-1 Higashi, Tsukuba, Ibaraki 305-8566

Received January 30, 2006; accepted March 9, 2006

Aptamers are known for their higher discriminating ability between closely related molecules and their requirement for only a small region for binding, as compared to an antibody. In the present studies, we have isolated a specific RNA aptamer against the influenza virus B/Johannesburg/05/1999 by an *in vitro* selection procedure. The aptamer bound efficiently to the HA of influenza B and required 5 mM $MgCl_2$ ion for its recognition. The aptamer not only distinguished HA derived from the influenza A virus, but also inhibited HA-mediated membrane fusion.

Key words: glycoprotein, hemagglutinin, human influenza B virus, lineage, membrane fusion, RNA aptamer.

Aptamers are rare functional nucleic acid motifs derived from libraries of nucleic acids by iterative rounds of selection and amplification in a process called "SELEX," systematic evolution of ligands and exponential enrichment. As the name implies, the aptamers are evolved for their specific binding and high affinity from combinatorial libraries of nucleic acid motifs. In the aptamer selection process, the oligonucleotide library is incubated with the target of interest and the buffer of choice at a given temperature. The bound oligonucleotides are then separated from the unbound oligonucleotides either by filtration on nitrocellulose filters or by an affinity process. By exploiting the SELEX method, several aptamers have been selected for a wide variety of targets, including simple ions, small molecules, peptides, proteins, organelles, viruses and even entire cells (*1*–*3*). Interestingly, the isolated aptamers display very high specificities (molecular discrimination as much as 10,000 fold) and target affinities (K_ds at subnanomolar levels), which are comparable to the affinities achieved by antibodies for antigens. Several applications of aptamers have been proposed and are presently in different stages of development.

In the past, several aptamers were developed against viral proteins including HIV-1 (Tat, Rev, reverse transcriptase, nucleoprotein, gp120, gag, and integrase), HTLV-1 (Rex and Tax), HCV (IRES, NS3, and RNA polymerase), and feline immunodeficiency (reverse transcriptase), as well as against whole human cytomegalovirus and RSV. These aptamers specifically inhibit their target functions both *in vitro* and *in vivo*. Recently, aptamers against hemagglutinin (HA) of human influenza A viruses have been reported (*4*–*6*). The major viral antigen, HA, is required for membrane fusion with host cells to mediate the early stage of influenza virus infection (*7*). In addition, HA is known to induce high levels of macrophage-derived chemokines and cytokines, which lead to the infiltration of inflammatory cells and severe hemorrhaging, especially when the HA is derived from a virulent strain (*8*). A DNA aptamer that efficiently blocks receptor binding has been reported (*4*). Recently, an RNA aptamer that discriminates the closely related HA derived from the H3N2 strain of influenza A virus and inhibits membrane fusion has also been reported (*6*).

In contrast to the influenza A viruses, the primary natural host of influenza B viruses is human. The influenza B viruses differ from influenza A viruses in their evolutionary characteristics, such as slower evolutionary rates, circulation of different lineages in the same population at a given time, and insertion and deletion mechanisms. Considering the importance of the diagnosis of influenza B infections, in the present study we have isolated specific RNA aptamers against the B/Johannesburg/05/1999 virus. The aptamer bind efficiently to the HA of influenza B and requires 5 mM $MgCl_2$ ion for its recognition. The aptamer not only distinguishes the HA derived from the influenza A virus, but also inhibits the HA-mediated membrane fusion.

EXPERIMENTAL PROCEDURES

Viral Stocks and Viral Proteins—The influenza viruses used in the present study were purified as described previously (*9*). To select the aptamer, we purified the target protein (consisting of the HA1/HA2 complex) from the viruses. The virus stock (1.2–1.4 mg viral protein in 1.5–2.0 ml PBS), containing about 30% sucrose, was diluted 1.5-fold with Tris buffer (50 mM Tris, 25 mM NaCl, 1 mM $CaCl_2$ pH 7.5), and centrifuged (for 30 min at 45,000 × *g* and 4°C) to remove the sucrose. The pellet was suspended in 0.25 ml of Tris buffer, mixed with 0.06 ml of 20% (w/w) Triton X-100, and incubated for 2 h at 37°C. After centrifugation for 30 min at 45,000 × *g* and 4°C, the supernatant was applied to an ion exchange column (Vivapure spin column, type S mini H, Sartorius AG, Germany). The protein eluted from the column was layered

*To whom correspondence should be addressed. Tel: +81-298-61-6085, Fax: +81-298-61-6095, E-mail: pkr-kumar@aist.go.jp

on a stepwise sucrose density gradient (20–60% w/w sucrose in PBS), and centrifuged for 20 h at 160,000 × *g* and 4°C. The sample was fractionated and examined by SDS-PAGE. The fractions containing the purified HA protein were collected and stored at –80°C until use. To prepare de-glycosidated HA, we carried out glycosidase digestions using two enzymes, *N*-glycosidase F (Roche) and endoglycosidase (New England BioLabs, USA). Initially, HA (23 mg) was mixed with *n*-decyl-β-D-maltopyranoside (69 mg) (Calbiochem, La Jolla, CA) in the presence of 20 mM phosphate buffer, pH 6.8, at 37°C for 2 h. After centrifugation at 130,000 × *g* at 4°C for 1 h, *N*-glycosidase F (250 units) and endoglycosidase (250,000 units) were added to the supernatant, and the reaction mixture was incubated for 24 h at 37°C. After the reaction was completed, the NaCl concentration was adjusted to 300 mM, and the mixture was centrifuged at 4,500 × *g* for 5 min at room temperature. The sample was then concentrated to 500 μl using an Amicon Centriprep filter (MWCO 50K). The de-glycosidated HA was separated from the glycosidases on a Gel-filtration column (Superose 12) in buffer (0.05% dodecyl maltoside, 10 mM Tris-HCl, 5 mM $MgCl_2$, pH 7.5). Fractions containing de-glycosidated-HA were pooled after their purity was analyzed by 10% SDS-PAGE.

Design of RNA Random Pool—SELEX libraries are designed to contain a central domain of a randomized sequence flanked by the 5′ and 3′ regions of invariable sequences. The ssDNA library *TCTAATACGACTCACTA-T A* GGAGCTCAGCCTTCACTGC–N74—GGCACCACGG-TCGGATCCAC, with 74-nucleotide contiguous random sequences, was synthesized and flanked by defined sequences, including the T7 promoter (in italics). The 5′ and 3′ defined sequences were 5′-*TCTAATACGACTCAC-TATA*GGAGCTCAGCCTTCACTGC-3′ and 5′-GTGGATC-CGACCGTGGTGCC-3′, respectively. Polymerase chain reaction (PCR) was performed with the DNA random library (1×10^{14} molecules), along with 0.25 μM each of the 5′- and 3′-primers. To preserve the abundance of the original library, the PCR was limited to eight cycles to avoid amplifying a skewed population of the random DNA library. The DNA library was converted into an RNA library by *in vitro* transcription using a T7 Ampliscribe kit (Epicentre Technologies), and used for selection.

In Vitro *Selection Procedure*—Selection was performed using 15 μg (~10^{14} RNA molecules) of the original RNA library in RNA binding buffer (50 mM Tris-HCl, pH 7.5, 25 mM NaCl, 5 mM $MgCl_2$) at a 20:1 molar ratio of RNA to protein. During the selection cycles, the HA concentration was reduced in the later cycles to select high affinity RNA. The RNA was briefly heated to 95°C and cooled to room temperature to form stable structures before the selection steps. In the selection cycles, tRNA (total tRNA from *E. coli*, Boehringer-Mannheim) was used as a non-specific competitor. After the RNA was incubated with HA at room temperature for 10 min, the protein-RNA complexes were filtered through a pre-wetted nitrocellulose acetate filter (HAWP filter, 0.45 μm, 13.0-mm, Millipore) fitted in a "Pop-top" filter holder (Nucleopore), and washed with 1-ml of binding buffer. The RNAs that were retained on the filter were eluted and recovered as described previously (*10*). The recovered RNAs were reverse-transcribed in 20 μl of a reaction mixture containing 50 mM Tris-HCl (pH 8.0), 40 mM KCl, 6 mM $MgCl_2$, 0.4 mM dNTPs, 2.5 μM primer (24.N30) and 5 U of AMV reverse transcriptase (Seikagaku). Nucleotides and enzymes were added after a denaturation and annealing step (2 min at 90°C followed by incubation at room temperature for 10 min). Reverse transcription was carried out for 1 h at 42°C. The resulting cDNA was amplified by PCR and used as the template to obtain RNA for the next round of selection. For amplification by the polymerase chain reaction (PCR), a 20 μl aliquot of the mixture after reverse transcription (cDNA reaction mixture) was diluted in 80 μl of a mixture for PCR [10 mM Tris-HCl (pH 8.8), 50 mM KCl, 1.5 mM $MgCl_2$, 0.1% Triton X-100, 5 U of Taq DNA polymerase (Takara), and 0.4 μM of each primer]. The reaction mixture was cycled at 94°C for 70 s, at 55°C for 50 s, and at 72°C for 70 s for as many cycles as needed to produce the product band with the correct size. The PCR product was precipitated in ethanol and used for transcription. Transcription *in vitro* was performed at 37°C for 3 h with a T7Ampliscribe kit (Epicentre Technologies). After treatment with DNase I, the reaction mixture was fractionated in an 8% denaturing polyacrylamide gel. The RNA was extracted from the gel, quantitated and used for the next cycle of selection and amplification.

We manipulated each selection cycle to ensure the specificity and high affinity of the binders to the HA of B/Johannesburg virus, including modifications of the ratio of RNA:HA, competitor concentrations, and buffer volumes. To remove the filter binders, which increased the background, we used Vivapure affinity columns and xenobind plates for selections in the 2nd, 4th and 7th generations, respectively. For selection using the Vivapure column, we allowed the HA to bind to the pre-wetted column in the presence of Tris buffer (50 mM Tris, 25 mM NaCl, 5 mM $MgCl_2$, pH 7.5). The column was washed with 600 μl of the same buffer, and then the aptamer and HA complex were made in the presence of tRNA, after the RNA obtained from the previous generation was denatured at 90°C for 20 min and the sample cooled to room temperature. The complex was incubated for about 10 min at room temperature, and then the unbound molecules were removed by four washes with 300 μl binding buffer. The bound RNAs were recovered in boiling 7 M urea solution, precipitated with ethanol, and regenerated by RT, PCR and *in vitro* transcription. In the 4th generation of selection, to remove the non-specific binders from the column, we passed the RNA-pool obtained from the 3rd generation through the same column in the absence of protein, and the flow-through RNA was used for selection.

For the Xenobind selection, we initially coated the wells with 5 μg of HA per milliliter of binding buffer and blocked the remaining sites with BSA (3% stock solution). The wells were then washed and used in the selections. In the selections, the RNA pool from the 6th cycle was denatured at 90°C for 2 min and allowed to cool at room temperature for 10 min to facilitate the equilibration of the different conformers. Then, the pooled RNA (1 μM) and tRNAs (80 μM) were mixed in 100 μl of binding buffer, loaded twice into the BSA coated wells, and incubated for 10 min at room temperature (25°C). The unbound RNAs were collected and loaded into wells coated with HA. The reaction mixture was incubated further for 10 min. The unbound molecules were discarded, and the wells were washed five times with 300 μl of binding buffer.

The bound RNAs were recovered using boiling 7 M urea solution, precipitated with ethanol and regenerated by RT, PCR and *in vitro* transcription.

Analysis of Aptamers—To obtain individual aptamers, the amplified PCR product from cycle 9 was ligated directly into the pCRII vector (Invitrogen), according to the manufacturer's protocol. DNA was isolated from individual clones by the alkaline-lysis method, and sequenced with a Dye Terminator Sequencing kit [Applied Biosystems Inc. (ABI)] on a DNA sequencer (Model 373A, ABI). The secondary structures of the aptamers were predicted by the BayesFold program (version 1.01). To evaluate the binding activities of the RNA pools from different selection cycles, as well as the individual aptamers, internally labeled RNA was prepared using 0.5 mCi/ml [α-^{32}P]CTP, and binding studies were performed using a filter binding assay similar to that reported previously (*11–13*). The binding and *in vitro* transcription conditions were similar to those used for selection, except for the molar ratio of RNA to HA protein (20 nM of RNA and 160 nM of HA). The filters were washed with 1 ml of binding buffer and air dried, and the radioactivity was quantitated with an image analyzer (BAS2000, Fuji Film). To ensure that the binding was specific, we added a 10-fold molar excess of tRNA to the binding reaction as a nonspecific competitor.

Binding Assay Using BIAcore—Kinetic measurements were conducted using BIAcore 2000 equipment with a streptravidin coated sensor-chip from BIAcore, Sweden. The association and dissociation kinetics of the selected aptamer against HA of B/Johannesburg and the sequence complementary to that of the selected aptamer were studied. To determine the affinity constants of the selected aptamers, we prepared the aptamers with 24-mer poly(A) nucleotides at the 3′-end, which could anneal to the complementary biotinylated oligo (dT) [5′-Biotin-$(T)_{24}$-3′]. To prepare this RNA extended at the 3′ end, we used two primers: a forward primer similar to that used in the selection, and a 3′ end primer [5′-$(T)_{24}$-GTGGATCCGACCGTGGTGCC-3′]. The double-stranded DNA template was generated by PCR and transcribed *in vitro*, as described above. Initially, the biotinylated oligo $(dT)_{24}$ was attached to the streptavidin (SA chip, BIAcore, Sweden) by dissolving the oligo in binding buffer (5 μM final concentration) and injecting it for 12–24 s (RU 1,000) at a flow rate of 5 μl/min. The excess or unbound biotinylated oligo was washed with binding buffer at a flow rate of 20 μl/min for 10 min. To analyze the binding kinetics of the aptamer, 20 μl of aptamer was injected (50 nM final concentration) at a flow rate of 2 μl/min for 10 min, which resulted in an increase of about 1,200 RU upon aptamer binding to the complementary biotinylated primer. Various concentrations of HA (8–80 nM) were injected into the flow cell at a flow rate of 20 μl/min for 3 min, and the binding kinetics were evaluated. The sensor chip was then washed with buffer solution, followed by 10 mM NaOH, before the next injection. The data were fit with a local fit of the kinetic simultaneous K_a/K_d model, assuming Langmuir (1:1) binding.

Phosphate Modification and Interference Analysis—In order to map the binding sites of the HA within the selected aptamer, a phosphate modification assay was performed. *In vitro* transcribed RNA was treated with calf intestine phosphatase for 1 h at 37°C, extracted with phenol, and precipitated with ethanol. The RNA was labeled with [γ-^{32}P] ATP and T4 polynucleotide kinase, electrophoresed in an 8% polyacrylamide/7 M urea gel, and eluted from the gel. The labeled RNA was allowed to fold into a tertiary structure by heating at 95°C for 2 min and slow cooling to room temperature. The 5′-end–labeled RNA (1,100 kcpm) was dissolved in buffer (20 mM HEPES, pH 8.0, 1 mM EDTA and 2.5 μg tRNA), and mixed with 5 μl of saturated *N*-nitroso-*N*-ethyl-urea in ethanol. After modification at 90°C for 2 min, the reaction was stopped by the addition of 15 μg carrier tRNA, and the sample was recovered by ethanol precipitation. To allow the formation of the aptamer-HA complex, 20 pmol of treated sample was denatured in 25 μl of selection binding buffer at 92°C for 2 min (magnesium ions added after denaturation), and allowed to cool at room temperature for 10 min. The complex was separated by passage through a nitrocellulose filter, and partially hydrolyzed in a solution (200 μl) of 100 mM Tris/HCl pH 9.0 at 50°C for 5 min. The RNA cleavage products were recovered by ethanol precipitation and loaded onto an 8% polyacrylamide/7 M urea gel. Aliquots of the alkaline hydrolysate of the aptamer and the sample digested with RNase T1 were co-electrophoresed for band identification. The gel was dried and exposed to X-ray film for autoradiography.

Inhibition of HA-Mediated Membrane Fusion by the Aptamer—The potential inhibitory effects of RNA aptamers on viral receptor–binding and membrane fusion were examined using fluorescently labeled virus and human red blood cell (RBC) ghost membranes. The viral membrane of Yamagata lineage B/Johannesburg/05/1999 was labeled with a fluorescent lipid probe, octadecyl rhodamine B (R18; Molecular Probes, Eugene, OR) as described by Hoekstra *et al.* (*14*). Human RBCs (type B+), obtained from a single healthy donor, were washed three times with PBS, and diluted to 1% (v/v) in PBS. The RBCs (0.2 ml) were allowed to attach to a poly-L-lysine–coated glass coverslip at 4°C for 15 min and then lysed to ghost membranes by three washes with ice-cold 5 mM sodium phosphate (pH 8.0). The ghost membranes were resealed in PBS containing 0.9 mM $CaCl_2$ and 0.49 mM $MgCl_2$

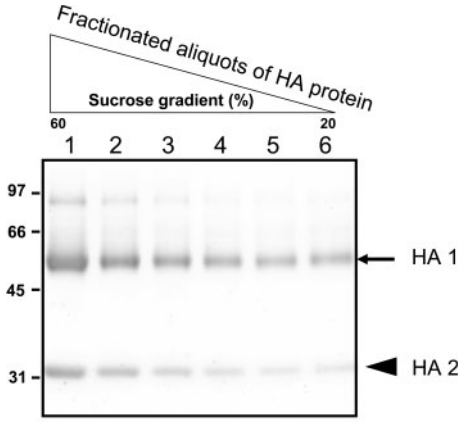

Fig. 1. **Purity analysis of HA derived from B/Johannesburg by SDS-PAGE (lanes 1–6: different fractions from the sucrose density gradient).** The positions of HA1 and HA2 are indicated.

for 30 min at 37°C, and were kept in Pipes buffer (5 mM Pipes-NaOH/145 mM NaCl, pH 7.5) on ice until use.

For the fusion inhibition assay, an image analysis of fusion at single virions in the presence of RNA aptamers was performed as follows. The R18-B/Johannesburg virus (0.05–0.1 μg total protein/ml) mixed with an RNA aptamer, Class A-20 (5 μM or 25 μM), in 0.2 ml of Pipes buffer containing magnesium ions supplemented with an RNase inhibitor (1 unit/μl SUPERase-in, Ambion, Austin TX) was added to ghost membranes on cover slips mounted in a metal chamber (*15*). After 3 min at 20°C, the unbound viral particles were removed by two washes with 0.1 ml Pipes buffer containing the RNase inhibitor (1 unit/μl), and the chamber was mounted on a laser-scanning microscope (LSM 510; Carl Zeiss, Oberkochen, Germany) equipped with a Planapochromat 63/1.4 NA objective. Time-lapse sequences of the fluorescence images at 1.5-s intervals were captured, and then to trigger the fusion activity of HA, the Pipes buffer was replaced with 0.2 ml of an acidic buffer (145 mM NaCl, 20 mM sodium citrate, 5 mM $MgCl_2$ 1 unit/μl of RNase inhibitor, pH 5.0). The fluorescence of R18 upon excitation with a 543-nm HeNe laser was imaged by using a 590-nm cut-off filter. To monitor the fluorescence intensities of individual fusing viral particles, regions of interest were drawn at the outlines of punctate fluorescence from R18-B/Johannesburg viruses on each recorded image file. The changes in the fluorescence intensity at individual regions were measured with NIH Image 1.61 software. Upon viral fusion with ghost membranes, lipid-intermixing between the viral and ghost membranes induces fluorescence dequenching of R18 (*16*, *17*). Thus, the response times before the fusion of single viral particles were determined by the timing of fluorescence flashes at single regions of interest on the microscopic images. The kinetics of vesicle fusion were obtained from the cumulative sums of the response time distributions.

Table 1. **Selection cycles and binding analysis to B/Johannesburg HA.**

Generation	RNA pool (μM)	Competitor [@] (μM)	Protein (μM)	Binding ability (%)[1]	No. of PCR cycles
1	8	80	0.4	0	6
2#	4	40	0.2	ND	10
3	2	40	0.2	ND	8
4#	1	40	0.2	ND	12
5	1	40	0.1	1.3	10
6	1	80	0.1	ND	8
7*	1	80	0.2	14	12
8	0.25	80	0.05	ND	8
9	0.5	160	0.05	27	8

[#]Vivapure column. [*]Xenobind plate. [@]tRNA. [1]Filter binding assay.

RESULTS AND DISCUSSION

Selection of a High-Affinity RNA Ligand to B/Johannesburg HA—Previously, high-affinity aptamers have been isolated against various nucleic-acid–binding proteins, proteins with unknown nucleic-acid–binding functions, and various small molecules (*18–23*). These studies revealed that aptamers can recognize various epitopes on protein surfaces, and can preferentially bind to active sites or recognition surfaces. HA is the receptor-binding

Class A (42%)

20

5'- GGGAGCUCAGCCUUCACUGC ACUCCGGCUGGUGGACGCGGUACGAGCAAUUUGUACCGGAUGGAUGUUCGGGCAGCGGUGUGGCAGGGAUGAGC GGCACCACGGUCGGAUCCAC -3'

Class B (33%)

11

5'- GGGAGCUCAGCCUUCACUGC AACGUGAGGGGGCCAGGUUGGAUCGGGUGUCGACGUGAUAGUGCGAUUGCUACUUGACGGAGGCGUAGCGAGUA GGCACCACGGUCGGAUCCAC -3'

Class C (17%)

25

5-' GGGAGCUCAGCCUUCACUGC CGUGAUAGUGCAACGGUGUAUGUUGGCUAGCUGCGCCAUGUCGAGCUGCAGCGACGGACCCUAGAUAGACCUUA GGCACCACGGUCGGAUCCAC -3'

Class D (8%)

6

5'- GGGAGCUCAGCCUUCACUGC CGAUACCGGCAAACCGAGACAUGCAAAAUGGGCCUUGGCUGCCCGUUUGAGAGCGAAAUGUCCAGCCUGUAUUA GGCACCACGGUCGGAUCCAC-3'

Fig. 2. **Primary sequence of selected aptamers against the HA of B/Johannesburg.** Underlined letters indicate the randomized region of the RNA.

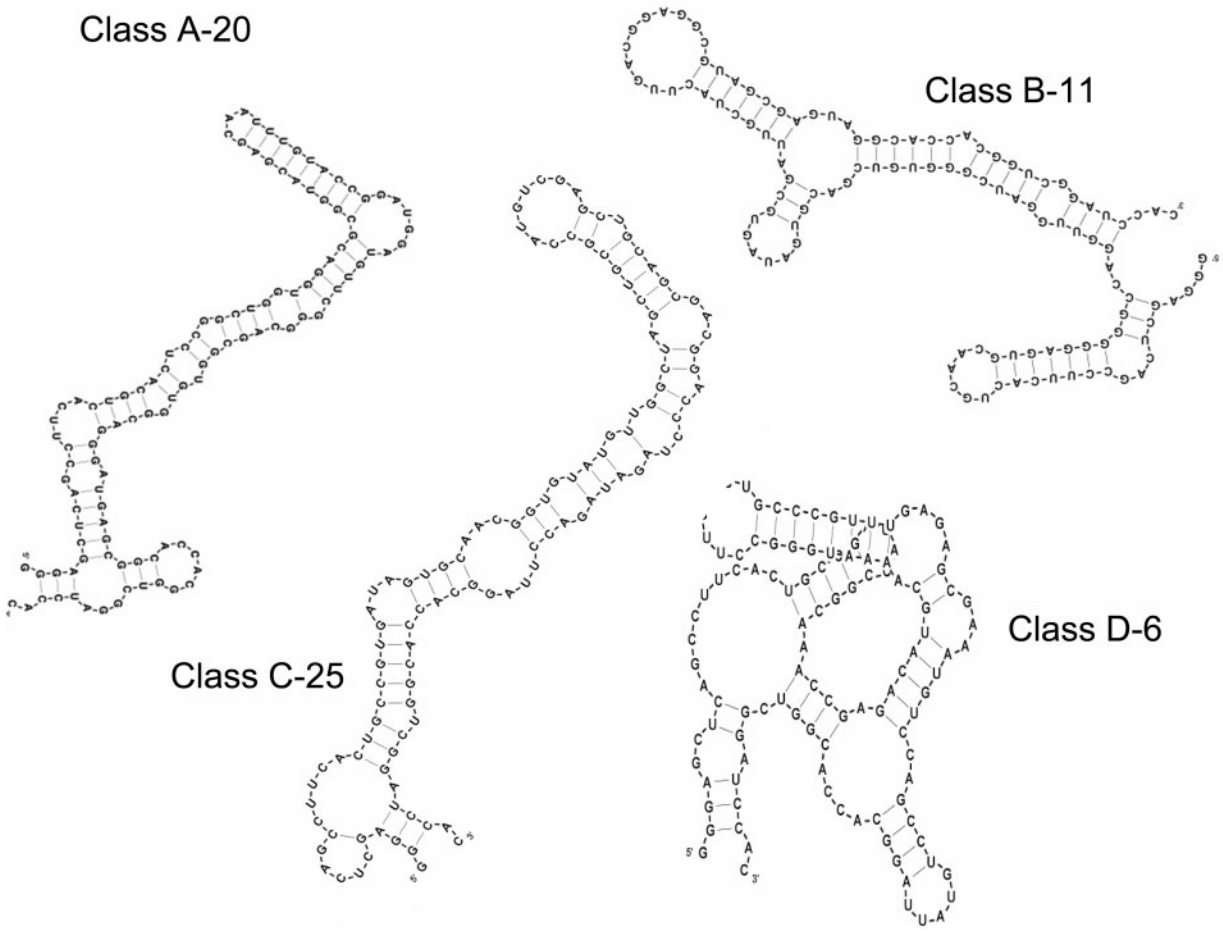

Fig. 3. **Predicted secondary structures of the selected aptamers (BayesFold version 1.01).**

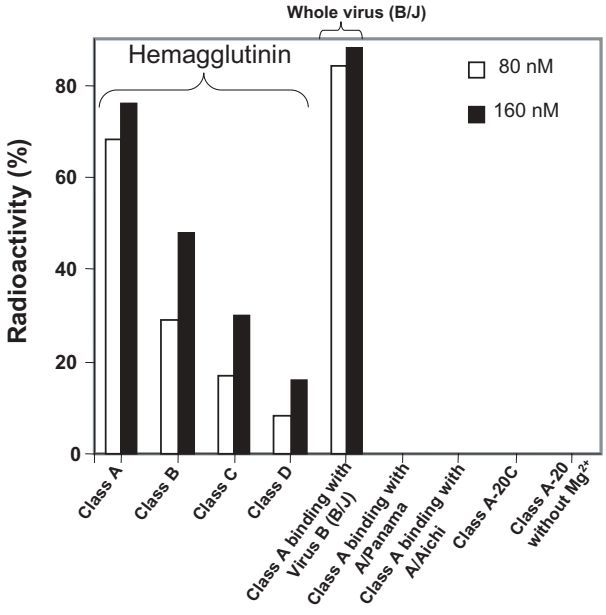

Fig. 4. **Filter binding assay to analyze the binding abilities of selected RNA aptamers against HA protein derived from either B/Johannesburg or other influenza viruses and the whole B/Johannesburg virus.** Binding reactions were performed at 80 nM (open bar) and 160 nM (filled bar) concentrations.

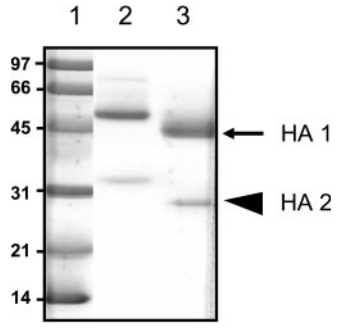

Fig. 5. **SDS-PAGE of the HA from B/Johannesburg.** Lane 1, Protein markers; lane 2, Non-deglycosylated HA; lane 3, de-glycosylated HA. The positions of HA1 and HA2 are indicated.

and membrane fusion glycoprotein of influenza virus, and thus it represents the target for infectivity-neutralizing antibodies. The membrane bound HA was purified from B/Johannesburg using the standard protocol and exhibited two subunits (HA1 and HA2) in SDS-PAGE analysis (Fig. 1). Fractions with pure proteins were pooled and dialyzed against storage buffer (50 mM Tris-HCl, 25 mM NaCl, 1 mM $CaCl_2$) containing 30% sucrose.

The selection of an aptamer against HA of human influenza virus B/Johannesburg/05/1999 is desirable because this kind of specific probe will greatly impact the

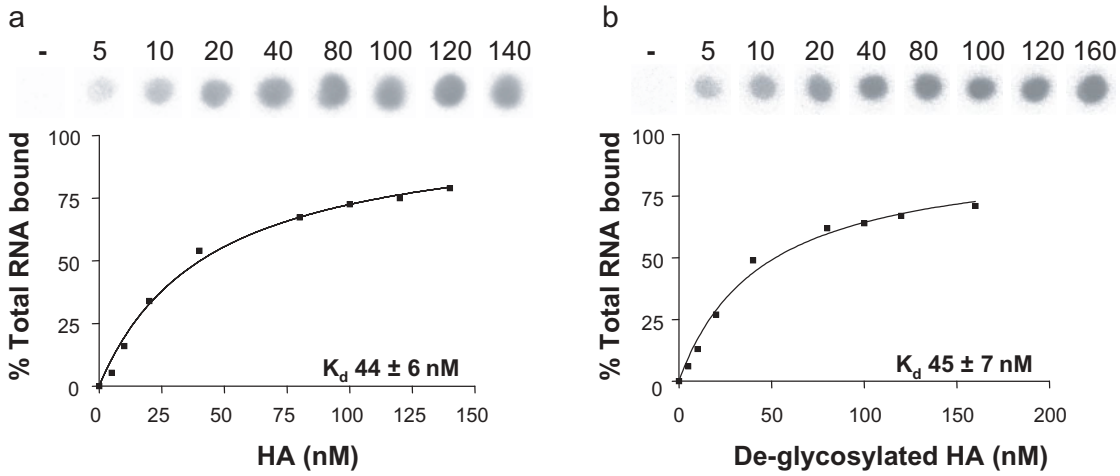

Fig. 6. **Binding analysis of the selected aptamer against HA (a) and deglycosylated HA (b).**

development of specific diagnostic reagents and inhibitors. The starting RNA repertoire was randomized over a 74-nucleotide stretch flanked by a fixed 38-nucleotide primer region at the 5′ end and a 20-nucleotide primer region at the 3′-end. This randomized pool contained approximately 10^{14} units of RNA species under our experimental conditions. For each selection, the RNA pool and HA were mixed and incubated for about 10 min, and then the free RNA was separated from the complexed-RNAs (HA-RNA complexes) by filtration or binding to a Vivapure column or xenoplate under the conditions required for the selection cycle. Bound RNAs were eluted and subsequently amplified by reverse transcription, PCR, and *in vitro* transcription. After nine rounds of selection and amplification, about 27% of the RNA pool was bound to HA (Table 1). No significant retention of the selected RNA pool occurred on the filter in the absence of HA, indicating that non-specific binders to filters were not co-isolated during the course of selection. After the ninth cycle of amplification and selection, PCR-derived molecules from the RNA pool were sub-cloned and sequenced. The sequenced clones were classified into 4 classes based on the sequence similarity and the population frequency, with decreasing percentage ranks of 42 > 33 > 17 > 8% (Fig. 2). Each class of aptamers was predicted to assume a different secondary structure (BayesFold version 1.01) (Fig. 3) and showed different binding abilities with HA (76, 48, 30 and 16%, respectively) (Fig. 4). The aptamers belonging to Class A were the most prolific, and the clone 20 in the Class A was selected for further studies.

Binding Specificity of the Selected Aptamer—The Class A-20 aptamer possesses high affinity for the cognate HA of B/Johannesburg, and was subjected to various analyses of its specificity and affinity, including the importance of the aptamer sequence, metal ion requirement, and the ability to distinguish other types of influenza viruses. The aptamer is able to bind the whole B/Johannesburg virus, indicating the recognition of HA protein (Fig. 4). The aptamer was also tested for its ability to distinguish the HA proteins derived from other sub-types of influenza viruses, which revealed that the selected aptamer binds specifically to the HA derived from the B/Johannesburg subtype. Next, to determine the importance of the Class A-20 aptamer

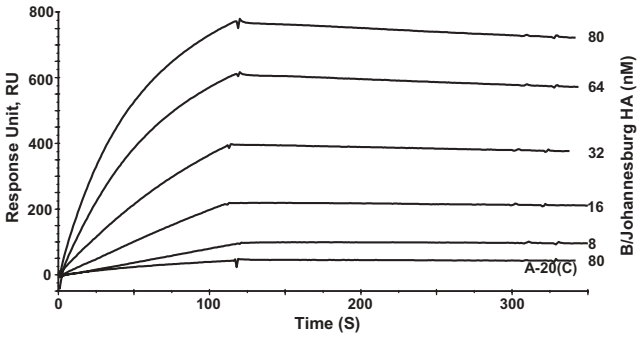

Fig. 7. **SPR-analysis of the binding kinetics of the aptamer-HA complex.** The aptamer was injected at a flow rate of 2 μl/min for 10 min (20 μl total volume; 50 nM final concentration). Sensogram runs with HA of B/Johannesburg/05/1999 injected into the flow cell at a flow rate of 20 μl/min for 3 min.

random region for HA binding, we prepared another aptamer (Class A-20C) containing the complementary sequence to the Class A-20 aptamer. The Class A-20C was unable to bind HA, demonstrating that the randomized region sequence is important for target protein binding (Fig. 4). Interestingly, when Mg^{2+} ions were not present in the binding buffer, the aptamer could not bind to its target. The inclusion of 5 mM of Mg^{2+} ion in the binding buffer restored its binding ability, indicating that magnesium ions probably facilitate the proper folding of the RNA (Fig. 4). Hemagglutinin is an *N*-glycosylated glycoprotein with a globular head and stem regions. Based on previous analyses of HA sequences from 1968 to 2002, the oligosaccharide chains display large variations in a number of different isolates (*24*). To address whether the aptamer specifically recognizes the residues of HA, but not the sugar chains of HA, we treated the HA with glycolytic enzymes using established protocols, and the resulting de-glycosylated HA (Fig. 5) was used for binding analysis. Under these conditions, major sugar chains are removed from HA. However, the complete removal of sugar chains from the HA was not analyzed. The Class A-20 aptamer bound with equal efficiency to both de-glycosylated and non-glycosylated HA, suggesting that the sugar-chains of the

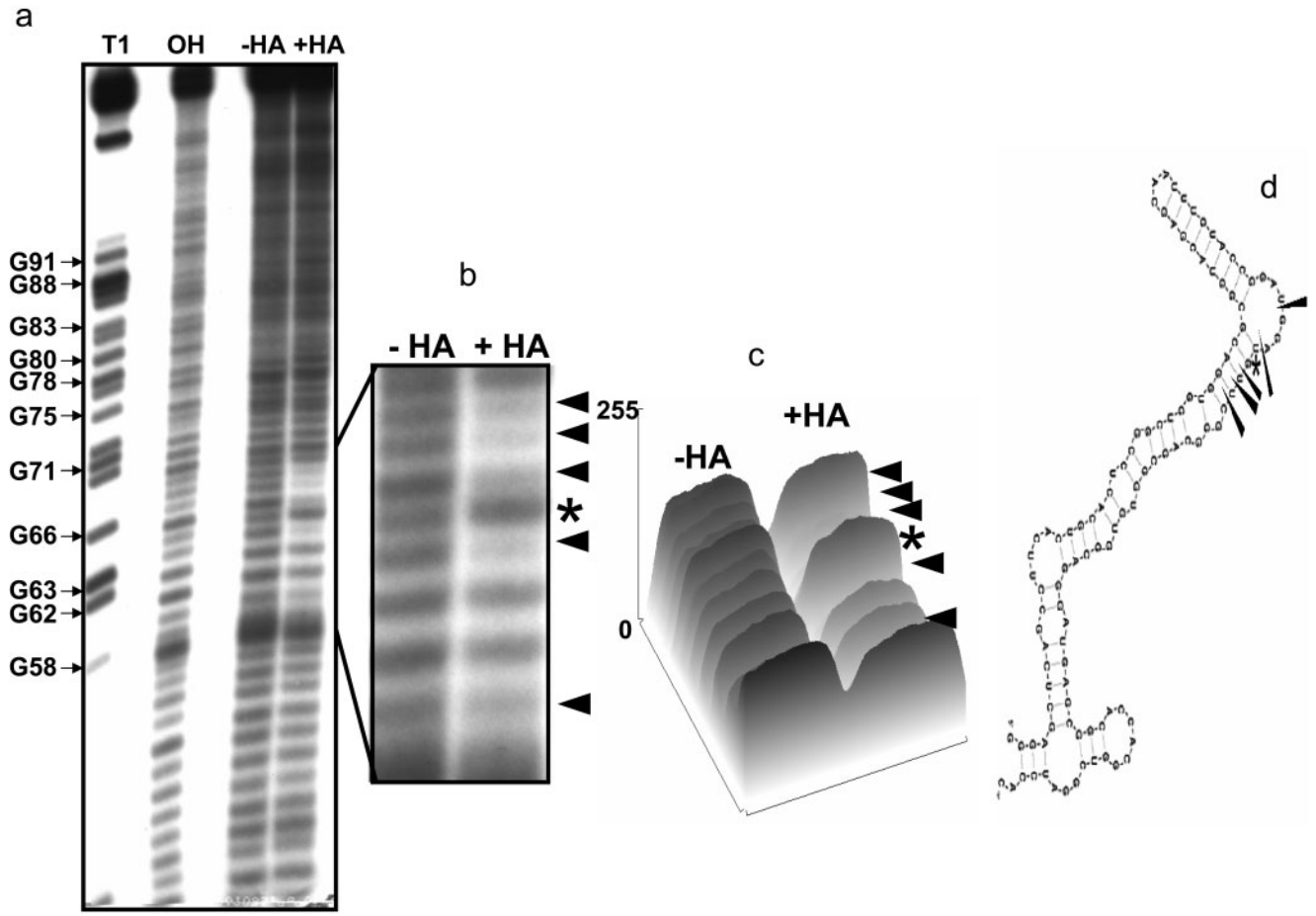

Fig. 8. **(a) Ethylnitrosourea mapping of interfering phosphates of the selected aptamer and HA binding.** The labeled ethylnitrosourea modified aptamer-HA complex was trapped on the nitrocellulose filter. After washing the complex with binding buffer, the filter was treated with mild alkaline solution. The RNA was recovered and loaded on the gel. The control RNA marker was prepared by partial nuclease digestion with RNase T1 (lane T1) and alkaline digestion (lane OH). **(b) Enlarged view.** Arrowheads and * indicate sites of phosphate interference and enhancement, respectively. **(c) Quantitative analysis of cleaved products.** The interferences are indicated as in (b). **(d) Secondary structure of the RNA (BayesFold version 1.01).** Phosphate Interference is indicated by either pointed triangles (arrowheads for reducing the signal) or stars (* for enhancing the signal).

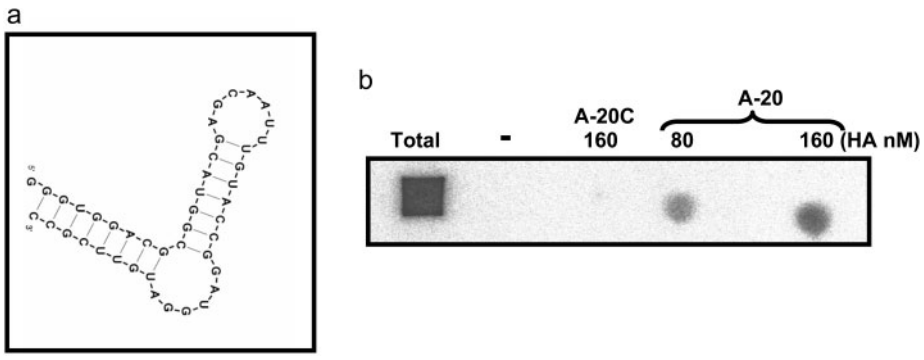

Fig. 9. **(a) Secondary structure of the A-20 mini aptamer (G at the 5′ end and two C residues at the 3′ end were added for efficient transcription and stability of the stem, respectively). (b) Filter binding assay to analyze the binding ability of the A-20 mini aptamer and and its complementary aptamer (A-20C) against HA of B/Johannesburg virus.**

HA protein may not be involved in aptamer recognition (Fig. 6, a and b).

Surface Plasmon Resonance Studies—To determine the binding kinetics of the aptamer-HA complex, we performed surface plasmon resonance (SPR) studies. The kinetics studies revealed that the aptamer binds to the HA with association (k_{on}) and dissociation constants (k_{off}) of 1.6×10^5 (M^{-1} s^{-1}) and 5×10^{-4} (s^{-1}), respectively. The equilibrium dissociation constant (K_d) for the above complex was 720 pM (Fig. 7). To evaluate the specificity of the aptamer

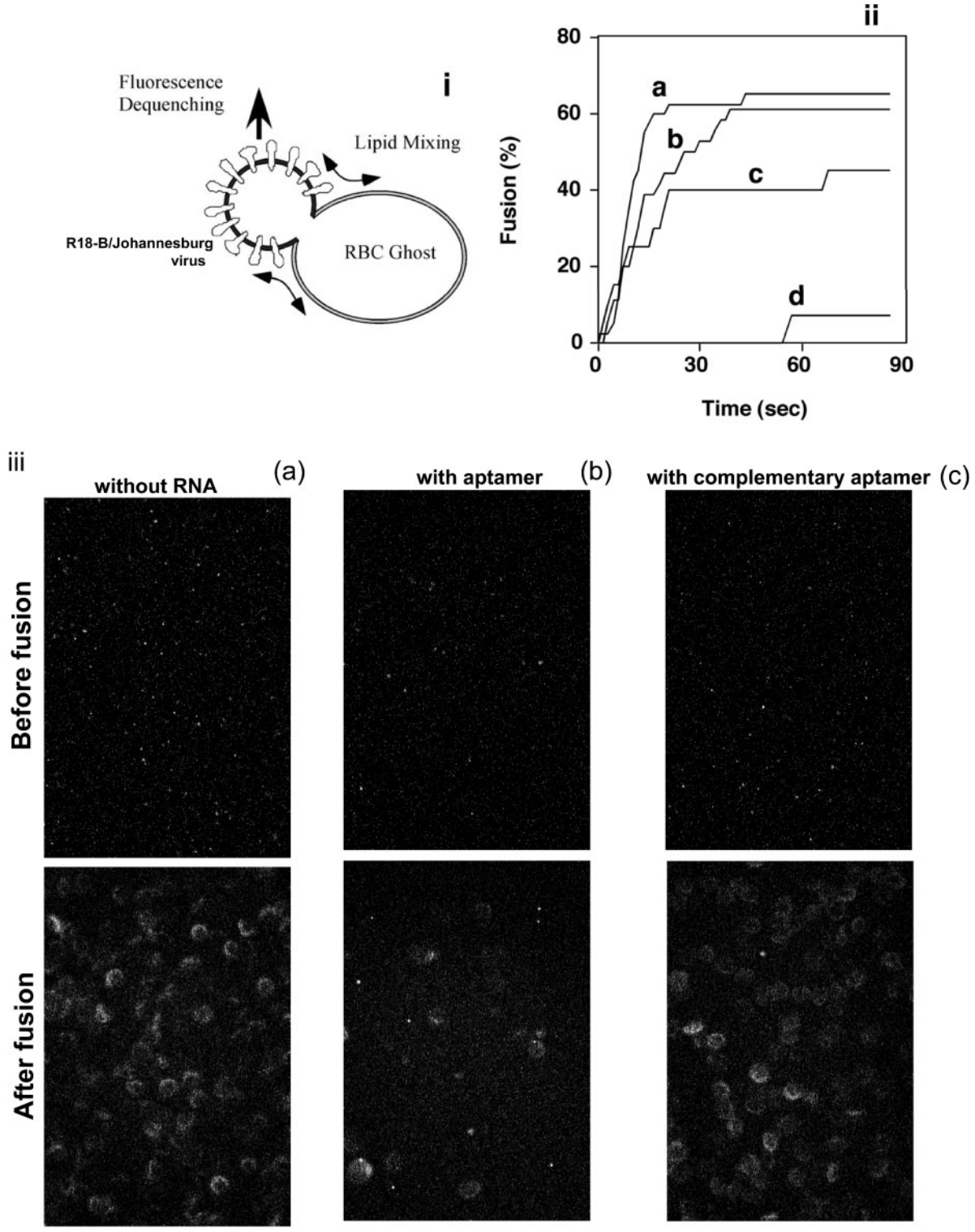

Fig. 10. **Inhibition of HA-mediated membrane fusion.** The inhibitory effect of the RNA aptamer on HA-mediated fusion was examined using a virus-RBC ghost fusion assay at pH 5.0 and 20°C. (i) A schematic drawing of the detection of fusion at individual virus particles. Viral membranes (B/Johannesburg strain) were labeled with a fluorescent lipid probe, R18. Low-pH dependent viral fusion with the target membranes, RBC ghosts, induces inter-membrane lipid mixing and dequenching of the R18 fluorescence. The increase in the fluorescence intensity at an individual virus particle was observed by fluorescence microscopy. (ii The viral fusion kinetics were determined by counting the number of fused virus particles at each time-point. a: without the addition of RNA. b: In the presence of 25 μM complementary RNA (Class A-20C). c and d: In the presence of 5 μM and 25 μM Class A-20 aptamer, respectively. Class A-20 inhibited the membrane fusion of virus-RBC ghost conjugates. (iii) Observation of fusion by fluorescent microscopy (a) HA-mediated membrane fusion in the absence of RNA. (b) Inhibition of HA-mediated membrane fusion by Class A-20 RNA. (c) Inhibition of HA-mediated membrane fusion by Class A-20C RNA.

sequence, we prepared a sequence complementary to that of the selected aptamer. This complementary sequence did not bind to the B/Johannesburg HA, suggesting the importance of the aptamer sequence.

Mapping and Minimal RNA Motif That Binds the B/Johannesburg HA—To identify important phosphates on the Class A-20 aptamer and to derive shorter aptamers for various analyses and applications, we used ENU-modification and interference analysis studies. Initially, the selected aptamer was labeled at the 5′ end and modified under denaturing conditions (92°C for 2 min) with ethylnitrosourea. Under these conditions, the ethylnitrosourea modifies the phosphates of the RNA at approximately one site/molecule. Since ethylnitrosourea reacts with phosphates and generates a phosphotriester in the RNA, it can be easily hydrolyzed by mild alkaline treatment. The alkylated RNA was allowed to bind to HA, and the complexed RNAs were separated from the free RNA by filtration and cleaved at the modified sites. The RNAs eluted from the nitrocellulose filters were loaded onto an 8% polyacrylamide gel to separate the cleaved products. In this process, the molecules that were modified at the phosphates necessary for binding to HA were lost, and these important phosphate regions could be visualized as a footprint on the sequencing gel. Comparisons of the band intensities of the samples of complexed and free RNA revealed the sites that are important for HA binding. Specifically, the phosphates at positions U61, A64, G66, U67 and U68 were found to interfere strongly with the HA, suggesting their importance for interactions with HA. In addition, position U65 is enhanced upon binding (Fig. 8, a and b). Although the base sequences were optimized during the selection process, the phosphates in random regions may also play an important role in efficient HA binding. Using ImageJ (free software from http://rsb.info.nih.gov), we scanned the hydrolyzed products obtained in the absence and presence of HA in the above phosphate interfering region, and observed the differences (Fig. 8, c and d). From the ENU-mapping study, we prepared a shorter derivative of the Class A-20 aptamer containing nucleotides 29–69 by *in vitro* transcription. This derivative was analyzed using a filter binding assay for binding to the B/Johannesburg HA. The binding results clearly indicated that nts 29 to 69 of Class A-20 are sufficient for binding to the B/Johannesburg virus or its HA, consistent with ENU mapping studies (Fig. 9). Thus, Class A-20 mini (41-mer) represents the smallest aptamer that binds specifically to the HA.

Inhibition of HA-Mediated Membrane Fusion by the Aptamer—Since the selected aptamer shows high affinity for the HA of an influenza virus, it is important to analyze the ability of the aptamer to inhibit the biological functions of HA. The HA of influenza virus mediates membrane fusion between the viral and target cellular membranes (*7*). Therefore, we analyzed the interaction of the fluorescently-labeled virus and a model target membrane, RBC ghosts, in the presence of aptamer Class A-20 (5 μM or 25 μM) and the complementary RNA Class A-20C, which allowed us to evaluate the ability of the aptamer to inhibit HA-mediated membrane fusion.

For a single-particle image analysis of membrane fusion, conjugates of R18-B/Johannesburg virus and RBC ghosts were observed by fluorescence microscopy. As shown schematically in Fig. 10-i, viral membrane fusion with RBC ghosts induced lipid mixing between the two membranes and reduced the R18 concentration in the membranes. The change was detected as an increase in the intensity of R18 fluorescence from individual virus particles, as previously demonstrated (*16*, *17*). The time-distribution of the fusion events thus measured was accumulated for several viral particle regions and used to obtain the viral fusion kinetics, as shown in Fig. 10-ii. The efficiency of viral fusion with RBC ghosts, 90s after a low-pH trigger, reached 68% without the addition of any RNA and 63% in the presence of 25 μM Class A-20C (Fig. 10-ii, a and b). In contrast, in the presence of 5 μM and 25 μM concentrations of the Class A-20 aptamer, the viral fusion efficiencies were suppressed to 45% and 7%, respectively (Fig. 10-ii, c and d), showing the efficient inhibition of viral fusion by the Class A-20 aptamer. Under neutral pH conditions (pH 7.5), individual virus particles were discerned as points of fluorescence, whereas the RBC ghosts bound to the viruses were invisible (Fig. 10-iii; upper panel). In the presence of the complementary RNA Class A-20C (25 μM), a low-pH trigger (pH 5.0) at 20°C induced lateral diffusion of R18 from the viruses to the RBC ghosts, and the RBC ghosts became fluorescent within 90s (Fig. 10-iii, c; lower panel). In contrast, in the presence of the aptamer Class A-20 (5 μM), lateral diffusion of R18 from the viruses to the RBC ghosts was not observed for most of the virus-ghost conjugates (Fig. 10-iii, b; lower panel).

Taken together, the present and previous selection studies on human influenza reveal that aptamers recognize HA with high affinity, and also have the interesting ability to distinguish specific strains of influenza viruses (*4–6*). In the present studies, we show that an aptamer (Class A-20) binds specifically to the HA of influenza B virus and fail to bind to HA belonging to influenza A viruses. Similar to other aptamers, the anti–HA influenza B aptamer inhibit membrane fusion. To understand how the aptamer prevents HA fusion with the membrane, it will be important to identify the aptamer binding region within the HA.

This work was supported by funds from the National Institute of Advanced Industrial Science and Technology (AIST) to P.K.R.K. S.C.B.G is supported by the Japan Society for the Promotion of Science (JSPS). We thank Dr. Hideaki Kumihashi for the kind gift of purified virus, and Ms. Hiromi Masuda and Ms.Takako Seki for the sequencing and the fusion analysis, respectively.

REFERENCES

1. Gold, L., Polisky, B., Uhlenbeck, O., and Yarus, M. (1995) Diversity of oligonucleotide functions. *Annu. Rev. Biochem.* **64**, 763–797
2. Osborne, S.E. and Ellington, A.D. (1997) Nucleic acid selection and the challenge of combinatorial chemistry. *Chem. Rev.* **97**, 349–370
3. Wilson, D.S. and Szostak, J.W. (1999) *In vitro* selection of functional nucleic acids. *Annu. Rev. Biochem.* **68**, 611–647
4. Jeon, S.H., Kayhan, B., Ben-Yadidia, T., and Arnon, R. (2004) A DNA aptamer prevents influenza infection by blocking the receptor binding region of the viral Hemagglutinin. *J. Biol. Chem.* **279**, 48410–48419

5. Misono, T.S. and Kumar, P.K.R. (2005) Selection of RNA aptamers against human influenza virus hemagglutinin using surface plasmon resonance. *Anal. Biochem.* **342**, 312–317
6. Gopinath, S.C.B., Misono, T., Kawasaki, K., Mizuno, T., Imai, M., Odagiri, T., and Kumar, P.K.R. (2006) An RNA aptamer that distinguishes between closely related human influenza viruses and inhibits hemagglutinin-mediated membrane fusion. *J. Gen. Virol.* **87**, 479–487
7. Skehel, J.J. and Wiley, D.C. (2000) Receptor binding and membrane fusion in virus entry: The influenza hemagglutinin. *Annu. Rev. Biochem.* **69**, 531–569
8. Kobasa, D., Takada, A., Shinya, K., Hatta, M., Halfmann, P., Theriault, S., Suzuki, H., Nishimura, H., Mitamura, K., Sugaya, N., Usui, T., Murata, T., Maeda, Y., Watanabe, S., Suresh, M., Suzuki, T., Suzuki, Y., Feldmann, H., and Kawaoka, Y. (2004) Enhanced virulence of influenza A viruses with the hemagglutinin of the 1918 pandemic virus. *Nature* **43**, 703–707
9. Kanaseki, T., Kawasaki, K., Murata, M., Ikeuchi, Y., and Ohnishi, S. (1997) Structural features of membrane fusion between influenza virus and liposome as revealed by quick-freezing electron microscopy. *J. Cell Biol.* **137**, 1041–1056
10. Kumar, P.K.R., Machida, K., Urvil, P.T., Kakiuchi, P.N., Vishnuvardhan, D., Shimotohno, K., Taira, K., and Nishikawa, S. (1997) Isolation of RNA aptamers specific to the NS3 protein of hepatitis C virus from a pool of completely random RNA. *Virology* **237**, 270–282
11. Yamamoto, R., Katahira, M., Nishikawa, S., Baba, T., Taira, K., and Kumar, P.K.R. (2000) A novel RNA motif that binds efficiently and specifically to the Tat protein of HIV and inhibits the trans-activation by Tat of transcription *in vitro* and *in vivo*. *Genes Cells* **5**, 371–388
12. Kumarevel, T.S., Fujimoto, Z., Karthe, P., Oda, M., Mizuno, H., and Kumar, P.K.R. (2004) Crystal strucuture of active HutP:A RNA binding protein that regulates hut operon in *Bacillus subtilis*. *Structure* **12**, 1269–1280
13. Kumarevel, T.S., Gopinath, S.C.B., Nishikawa, S., Mizuno, H., and Kumar, P.K.R. (2004) Identification of important chemical groups of the hut mRNA for HutP interactions that regulate the hut operon in *Bacillus subtilis*. *Nucleic Acids Res.* **32**, 3904–3912
14. Hoekstra, D., de Boer, T., Klappe, K., and Wilschut, J. (1984) Fluorescence method for measuring the kinetics of fusion between biological membranes. *Biochemistry* **23**, 5675–5681
15. Mizuno, T., Kawasaki, K., and Miyamoto, H. (1992) Construction of a thermotaxis chamber providing spatial or temporal thermal gradients monitored by an infrared video camera system. *Anal. Biochem.* **207**, 208–213
16. Georgiou, G.N., Morrison, I.E., and Cherry, R.J. (1989) Digital fluorescence imaging of fusion of influenza virus with erythrocytes. *FEBS Lett.* **250**, 487–492
17. Lowy, R.J., Sarkar, D.P., Chen, Y., and Blumenthal, R. (1990) Observation of single influenza virus-cell fusion and measurement by fluorescence video microscopy. *Proc. Natl. Acad. Sci. USA* **87**, 1850–1854
18. Tuerk, C., MacDougal, S., and Gold, L. (1992) RNA pseudoknots that inhibit human immunodeficiency virus type 1 reverse transcriptase. *Proc. Natl. Acad. Sci. USA* **89**, 6988–6992
19. Paborsky, L.R., McCurdy, S.N., Griffin, L.C., Toole, J.J., and Leung, L.L.K. (1993) The single-stranded DNA aptamer-binding site of human thrombin. *J. Biol. Chem.* **268**, 20808–20811
20. Conrad, R., Keranen, L.M., Newton, A.C., and Ellington, A.D. (1994) Isozyme-specific inhibition of protein kinase C by RNA aptamers. *J. Biol. Chem.* **269**, 32051–32054
21. Jellinek, D., Green, L.S., Bell, C., and Janjinc, N. (1994) Inhibition of binding by high-affinity RNA ligands to vascular endothelial growth factor. *Biochemistry* **33**, 10450–10456
22. Kubik, M.F., Stephens, A.W., Schneider, D.A., Marlar, R., and Tassett, D. (1994) High-affinity RNA ligands to human α-thrombin. *Nucleic Acids Res.* **22**, 2619–2626
23. Brown, D. and Gold, L. (1995) Selection and characterization of RNAs replicated by Qβ replicase. *Biochemistry* **34**, 14775–14782
24. Abe, Y., Takashita, E., Sugawara, K., Matsuzaki, Y., Muraki, Y., and Hongo, S. (2004) The effect of the N-glycosylation on the biological activities of influenza A/H3N2 hemagglutinin. In *Options for the Control of Influenza V* (Kawaoka, Y., ed.) pp. 214–217, International Congress Series 1263, Japan